Inorg. Chem. **2005**, *44*, 9779–9786

Cadmium(II) and Zinc(II) Complexes of Pyrrole-Appended Oxacarbaporphyrin: A Side-on Coordination Mode of *O*-Confused Carbaporphyrin

Miłosz Pawlicki, Lechosław Latos-Grażyński,* and Ludmiła Szterenberg

Department of Chemistry, University of Wrocław, 14 F. Joliot-Curie Street, Wrocław 50 383, Poland

Received July 25, 2005

A pyrrole adduct of 5,20-diphenyl-10,15-di(*p*-tolyl)-2-oxa-21-carbaporphyrin [(H,pyr)*OC*P*H*]H_2 reacted with sodium ethanolate to yield 5,20-diphenyl-10,15-di(*p*-tolyl)-3-ethoxy-3-(2′-pyrrol)-2-oxa-21-carbaporphyrin [(EtO,pyr)*OC*P*H*]H_2. Subsequently, "true" *O*-confused oxaporphyrin with a pendant pyrrole ring [(pyr)*OC*P*H*]H was formed by the addition of acid to [(EtO,pyr)*OC*P*H*]H_2, which triggered an ethanol elimination. In the course of this process, the tetrahedral–trigonal rearrangements originated at the C(3) atom. Insertion of zinc(II), cadmium(II), and nickel(II) into [(pyr)-*OC*P*H*]H yielded [(pyr)*OC*P*H*]$Zn^{II}Cl$, [(pyr)*OC*P*H*]$Cd^{II}Cl$, and [(pyr)*OC*P]Ni^{II}. The formation of [(pyr)*OC*P]Ni^{II} was accompanied by the C(21)H dehydrogenation step. The nickel(II) ion of [(pyr)*OC*P]Ni^{II}, coordinated to a dianionic macrocyclic ligand, is bound by three pyrrolic nitrogens and a trigonally hybridized C(21) atom of the inverted furan. The pyrrole-appended *O*-confused carbaporphyrin acts as a monoanionic ligand toward zinc(II) and cadmium-(II) cations. Three nitrogen atoms and the C(21)H fragment of the inverted furan occupy equatorial positions. In ^{1}H NMR spectra, the unique inner C(21)H resonances of the inverted furan ring are located at 0.15 ppm for [(pyr)-*OC*P*H*]$Zn^{II}Cl$, and at 0.21 ppm for [(pyr)*OC*P*H*]$Cd^{II}Cl$. The proximity of the furan fragment to the metal ion induces direct scalar couplings between the spin-active nucleus of the metal ($^{111/113}$Cd) and the adjacent ^{1}H nucleus. The interaction of the metal ion and C(21)H was also reflected by significant changes in carbon chemical shifts ([(pyr)-*OC*P*H*]$Zn^{II}Cl$, 78.3 ppm; [(pyr)*OC*PH]$Cd^{II}Cl$, 81.4 ppm; the free base, 101.3 ppm). The density functional theory (DFT) has been applied to model the molecular structures of zinc(II) and cadmium(II) complexes of *O*-confused oxaporphyrin with an appended pyrrole ring. The Cd···C(21) distance in the optimized structure exceeds the typical Cd–C bond lengths, but is much shorter than the corresponding van der Waals contact.

Introduction

Inverted porphyrin **1** (*N*-confused porphyrin, 5,10,15,20-tetraaryl-2-aza-21-carbaporphyrin)[1,2] and its derivatives have revealed a remarkable tendency to stabilize peculiar organometallic compounds.[3−6] At present, one can notice that organometallic chemistry in the macrocyclic environment extends beyond the inverted porphyrin, and includes a whole class of macrocyclic ligands, called carbaporphyrinoids. In general, carbaporphyrinoids are porphyrin analogues that possess at least one CH unit in place of a pyrrolic nitrogen in the coordination core, and which are potentially suited for accommodating a large variety of metal ions. For instance, the coordination properties of 6,11,16,21-tetraarylbenziporphyrin,[7−9] 8,19-dimethyl-9,13,14,18-tetraethyloxybenziporphyrin,[10] azuliporphyrins,[11] and benzocarbaporphyrin[12] have been investigated. 5,10,15,20-Tetraphenyl-*p*-benziporphyrin is a carbaporphyrinoid with a *p*-phenylene

* To whom correspondence should be addressed. E-mail: LLG@wchuwr.chem.uni.wroc.pl.

(1) Chmielewski, P. J.; Latos-Grażyński, L.; Rachlewicz, K.; Głowiak, T. *Angew. Chem., Int. Ed.* **1994**, *33*, 779.
(2) Furuta, H.; Asano, T.; Ogawa, T. *J. Am. Chem. Soc.* **1994**, *116*, 767.
(3) Latos-Grażyński, L. Core Modified Heteroanalogues of Porphyrins and Metalloporphyrins. In *The Porphyrin Handbook*; Kadish, K. M., Smith, K. M., Guilard, R., Eds.; Academic Press: New York, 2000; pp 361−416.
(4) Furuta, H.; Maeda, H.; Osuka, A. *Chem. Commun.* **2002**, 1795.
(5) Srinivasan, A.; Furuta, H. *Acc. Chem. Res.* **2005**, *38*, 10.
(6) Harvey, J. D.; Ziegler, C. J. *Coord. Chem. Rev.* **2003**, *247*, 1.
(7) Stępień, M.; Latos-Grażyński, L. *Chem.—Eur. J.* **2001**, *7*, 5113.
(8) Stępień, M.; Latos-Grażyński, L.; Szterenberg, L.; Panek, J.; Latajka, Z. *J. Am. Chem. Soc.* **2004**, *126*, 4566.
(9) Stępień, M.; Latos-Grażyński, L. *Acc. Chem. Res.* **2005**, *38*, 88.
(10) Stępień, M.; Latos-Grażyński, L.; Lash, T. D.; Szterenberg, L. *Inorg. Chem.* **2001**, *40*, 6892.
(11) Graham, S. R.; Ferrence, G. M.; Lash, T. D. *Chem. Commun.* **2002**, 894.

10.1021/ic051238x CCC: $30.25
Published on Web 11/23/2005

Scheme 1. Heteroatom-Confusion Concept

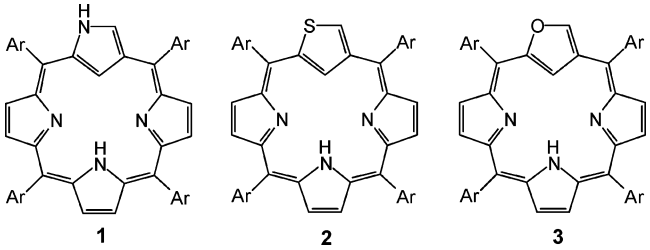

Scheme 2. Derivatives of *O*-Confused Porphyrins

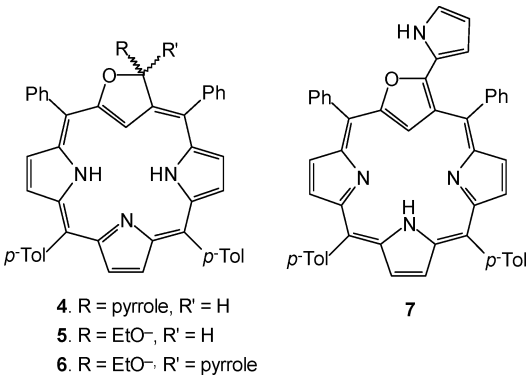

ring embedded in the tripyrrolic framework that may be considered to have two adjacent CH units in the macrocyclic core. Significantly, *p*-benziporphyrin forms a complex with cadmium(II) and nickel(II) to reveal an unprecedented η^2 Cd(II)−arene and η^2 Ni(II)−arene interaction.[8,13]

In the construction of a nontrivial macrocyclic environment for organometallic chemistry, we can apply a heteroatom confusion (*X*-confusion) concept, originally exemplified by a porphyrin−2-aza-21-carbaporphyrin couple.[1,2] Thus, interchanging a β-methine group with a heteroatom of 21-heteroporphyrin transforms the regular porphyrin into its *X*-confused isomer (**1**, **2**, and **3**, respectively) classified as carbaporphyrinoid by virtue of a (CNNN) coordination core. These molecules, although porphyrin-like in character, are expected to have fundamentally different electronic and coordination properties.

In our initial studies, we have reported the synthesis of *S*-confused thiaporphyrin **2**.[14] Following this direction, we have obtained a group of carbaporphyrins or metallocarbaporphyrins, constructed using the *O*-confusion strategy (Scheme 2).[15] The extremely reactive periphery of 3-oxa-21--carbaporphyrin **3** facilitates a formation of addition products (pyrrole, **4**; ethanol, **5**) in reasonable yields.[15,16] To date, the synthesis and characterization of the free base related to **3** has been achieved in a single case of **4**, which can be formally considered as an effect of 2-oxa-3-(2′-pyrrolyl)-5,10,15,20-tetraphenyl-21-carbaporphyrin [(pyr)*OCPH*]H **7** hydrogenation.[15,17] The macrocycles **6** and **7** have been solely characterized as ligands at the respective nickel(II) (**7**-Ni), palladium(II) (**7**-Pd) , and silver(III) (**4**-Ag, **6**-Ag, or **7**-Ag) complexes (Scheme 3).

These carbaporphyrinoids reveal the peculiar flexibility of their molecular and electronic structures, which readily adjust the anionic character of a coordination core to an oxidation state of the metal ion. Modifications are readily triggered by the addition and/or elimination of a nucleophile at the perimeter furan carbon. Tetrahedral−trigonal rearrangements originate at the C(3) atom, and control a crucial pyrrole contribution to the macrocyclic conjugation.[15]

The further exploration of **4**, **5**, **6**, and **7** as flexible macrocyclic organometallic ligands implies their isolation in free base forms. Recently, we have described the synthesis and spectroscopic characterization of 2-oxa-21-carbaporphyrin derivatives without appended pyrrole linked to C(3), including the inherently reactive, true *O*-confused 2-oxa-21-carbaporphyrin [(H)*OCPH*]H **3**.[16] At this stage of exploration, we have readily realized that the coordinating properties of true *O*-confused oxaporphyrin, which contains the sp^2 hybridized C(3) carbon atom, can be investigated, provided that the stable 3-substituted derivatives of **3** will be used. In light of this objective, *O*-confused oxaporphyrin with appended pyrrole, i.e., 2-oxa-3-(2′-pyrrolyl)-5,10,15,20-tetraphenyl-21-carbaporphyrin **7**, is of particular importance. The formation of an inverted porphyrin with a pendant pyrrole ring was also reported.[18] Potentially, **7** may act as a mono- or dianionic ligand after the dissociation of NH or NH and C(21)H protons, respectively. The dianionic nature of **7** has already been revealed in the coordination of nickel(II) (**7**-Ni) or silver(III) (**7**-Ag) (Scheme 3).[15]

Here, the coordination of zinc(II) and cadmium(II) has been explored. For the very first time, *O*-confused oxaporphyrin has been found to act as a monoanionic ligand. Consequently, an unprecedented side-on coordination mode of *O*-confused carbaporphyrin has been detected, which affords an interaction between the metal ion and the C(21)H unit. Previously, we have determined that the adjacency of the NMR-active metal ion and the CH unit results in profound changes in NMR parameters.[8,13,19,20] Here, the detected couplings with the spin-active $^{111/113}$Cd have been applied as a proof for the unique interaction with the CH unit of the inverted furan. Such couplings are usually classified as "through-space" or "nonbonding", because their magnitude cannot be rationalized in terms of the network of formal bonds in the molecule.[21,22]

(12) Lash, T. D.; Rasmussen, J. M.; Bergman, K. M.; Colby, D. A. *Org. Lett.* **2004**, *6*, 549.
(13) Stępień, M.; Latos-Grażyński, L. *J. Am. Chem. Soc.* **2002**, *124*, 3838.
(14) Sprutta, N.; Latos-Grażyński, L. *Tetrahedron Lett.* **1999**, *40*, 8457.
(15) Pawlicki, M.; Latos-Grażyński, L. *Chem.—Eur. J.* **2003**, *9*, 4650.
(16) Pawlicki, M.; Latos-Grażyński, L. *J. Org. Chem.*, **2005**, *70*, 9123.
(17) From now on, we will use the symbol (H)*OCP* to denote the hypothetical dianion obtained from the *O*-confused oxaporphyrin **3** by abstraction of a pyrrolic NH proton and the C-bound proton H(21). The groups attached to the C(3) atom will be indicated by a prefix enclosed in parentheses. The group attached to C(21) will appear as a suffix. A similar description will be used for **4**, formally a pyrrole addition product of **3**. Here, the hypothetical trianion is noted as (H,pyr)*OCP*. Consequently, the following acronyms correspond to neutral structures [(H)*OCPH*]H **3**, [(H,pyr)*OCPH*]H_2 **4**, [(H,EtO)-*OCPH*]H_2 **5**, [(pyr,EtO)*OCPH*]H_2 **6**, and [(pyr)*OCPH*]H **7**.
(18) Schmidt, I.; Chmielewski, P. J. *Tetrahedron Lett.* **2001**, *42*, 1151.
(19) Hung, C.-H.; Chang, F.-C.; Lin, C.-Y.; Rachlewicz, K.; Stępień, M.; Latos-Grażyński, L.; Lee, G.-H.; Peng, S.-M. *Inorg. Chem.* **2004**, *43*, 4118.
(20) Rachlewicz, K.; Wang, S.-L.; Peng, C.-H.; Hung, C.-H.; Latos-Grażyński, L. *Inorg. Chem.* **2003**, *42*, 7348.
(21) Hilton, J.; Sutcliffe, L. H. *Prog. NMR Spectrosc.* **1975**, *10*, 27.

Scheme 3. Coordination Modes of Pyrrole-Appended *O*-Confused Porphyrins

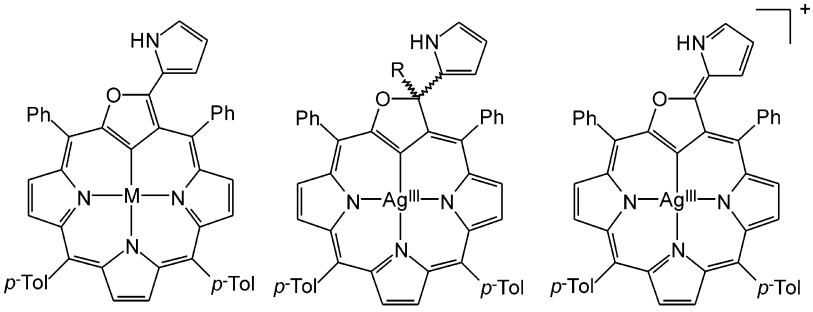

Results and Discussion

Synthesis of [(EtO,pyr)*OC*P*H*]H$_2$. As described previously, the condensation of 2,4-bis(phenylhydroxymethyl)-furan with pyrrole and *p*-tolylaldehyde (1:3:2 molar ratio) via a one-pot, two-step, room-temperature synthesis yielded a pyrrole adduct of 5,20-diphenyl-10,15-di(*p*-tolyl)-2-oxa-21-carbaporphyrin **4**.[15] Originally, we focused our attention on the coordinating properties of **4**. In terms of present studies, the facile transformation of [(H,pyr)*OC*P]Ag^{III} **4**-Ag into [(C_2H_5O,pyr)*OC*P]Ag^{III} **6**-Ag (Scheme 3) via ethoxy substitution is of particular interest.[15] Significantly, a subsequent acidification of **6**-Ag yielded the silver(III) complex of true *O*-confused oxaporphyrin, albeit with appended pyrrole ring [(pyr)*OC*P]Ag^{III}]$^+$ **7**-Ag. Presumably, the silver(III) cation activates the ligand perimeter, allowing for the facile changes centered at the C(3) position. In principle, an extrusion of silver from **6**-Ag or **7**-Ag using strong acid should afford **7**, which was never the case despite several attempts.

The pyrrole adduct of 2-oxa-21-carbaporphyrin **4** undergoes a substitution when treated with ethoxide in ethanol. In comparison, to synthesize **7**-Ag from **6**-Ag,[15] we carried out the reaction, which requires an elevated temperature, in a boiling solution of sodium ethoxide. The chromatographic workup of the resulting mixture gave **6** practically in quantitative yield. The structure of **6** was confirmed by a combination of high-resolution mass spectrometry and NMR spectroscopy.

Spectroscopic Characterization of [(EtO,pyr)*OC*P*H*]H$_2$ (6). The electronic spectrum of [(EtO,pyr)*OC*P*H*]H$_2$ **6** (Figure 1, blue), with its intense Soret-like band (433 nm in CH_2Cl_2) and a set of bands in the Q region, reflects the aromatic character of this new ligand.

The ^{1}H NMR spectrum of **6** (Figure 2, trace A) shows three AB patterns assigned to three pyrrole rings at the position expected for an aromatic carbaporphyrinoid. The complete assignments of all ^{1}H NMR resonances for **6**, shown in Figure 2, have been obtained by means of 2D ^{1}H NMR COSY and NOESY experiments using the unique NOE correlation between CH_2 and *o*-H(5-phenyl) as a starting point. The ethoxy group and pyrrole ring are bound to the tetrahedral carbon atom, which differentiates two sides of the macrocycle. At the same time, the ^{13}C chemical shift (111.8 ppm) is consistent with the tetrahedral hybridization of C(3), which is linked to two oxygen atoms. The presence of the ethoxy substituent is manifested by the diastereotopically split methylene multiplets at 3.86 and 3.35 ppm (Figure 2, trace A, inset). Essentially, the molecule **6** demonstrates aromaticity due to the typical 18-π-electron delocalization pathway (Scheme 3). The strongly upfield positions of the H(21) (−5.55 ppm) and inner NH (−2.82, −3.07 ppm, 223 K) resonances are readily accounted for by the ring-current effect.

True *O*-Confused Oxaporphyrin with a Pendant Pyrrole Ring [(pyr)*OC*P*H*]H (7). Gradual addition of TFA to a solution of **6** in dichloromethane transforms the neutral form of **6** into the violet protonated form **7**-H_2, i.e., {[(pyr)-*OC*P*H*]H_3}$^{2+}$ **7**-H_2 (Scheme 4). Titration followed by UV−vis spectroscopy proceeds with well-defined isosbestic points, and the final spectrum of **7**-H_2 is shown in Figure 1. The strong Soret band of **6** disappeared. Several bands in the region typically assigned to the Soret-like band of aromatic carbaporphyrinoids, however, could be detected, but their low extinction coefficients, ca. $\epsilon = 8 \times 10^3$, imply lowering of the aromatic character of **7**-H_2.

The ^{1}H NMR spectroscopic titration of **6** with TFA carried out in CD_2Cl_2 at 298 K demonstrated a gradual growth of a separate set of resonances assigned directly to **7**-H_2 (Figure 2, Scheme 4). A new aromatic carbaporphyrinoid **7**-H_2 has been formed via an exocyclic C(3)−O bond cleavage, presumably activated by protonation of the ethoxy group and followed by elimination of ethanol. In the course of this

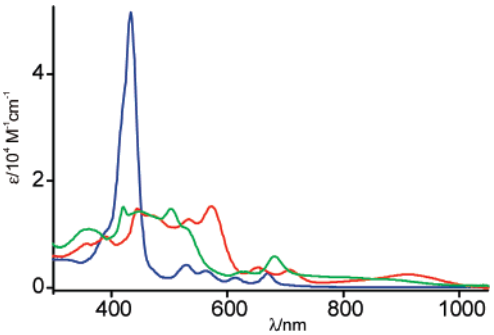

Figure 1. Electronic spectra of **6** (blue), **7**-H_2 (red), and **7** (green) in CH_2Cl_2.

(22) Contreras, R. H.; Facelli, J. C. *Annu. Rep. NMR Spectrosc.* **1993**, *27*, 255.

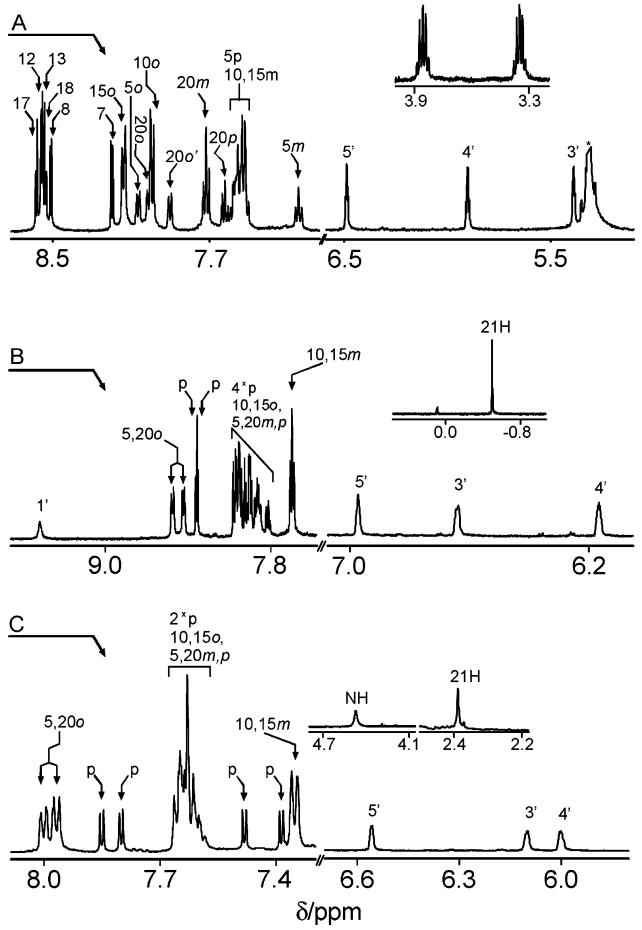

Figure 2. ^{1}H NMR spectra of (A) **6**, (B) **7**-H_2, and (C) **7** (dichloromethane-d_2, 298 K). The diastereotopic splitting of the CH_2 resonances of 3-ethoxide of **6** is shown in trace A. Insets B and C present the NH and H(21) resonances.

Scheme 4. Reactivity of Oxacarbaporphyrin with Appended Pyrrole

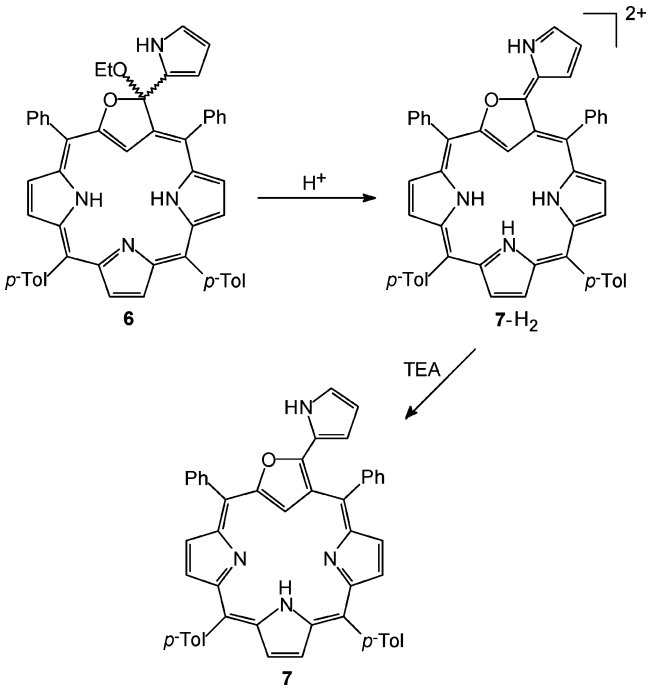

reversible process, the tetrahedral−trigonal rearrangements originate at the C(3) atom. The diastereotopically split ethoxy methylene multiplet of **6** has been replaced by a quartet of the free ethanol. Importantly, 1 equiv of ethanol was released, as confirmed by careful integration of the alcohol resonances with respect to those of **7**-H_2. The careful neutralization of **7**-H_2 with triethylamine produced **7**.

The ^{1}H NMR spectrum of **7**-H_2 (Figure 2, trace B) shows three AB patterns assigned to three pyrrole rings. The NH groups gave three broad singlets at 4.16, 4.12, and 4.00 ppm (233 K), i.e., upfield with respect to the NH resonance of unsubstituted pyrrole. The unique inner C(21)H resonance of the inverted furan ring is located at −0.51 ppm, i.e., upfield with respect to the corresponding 3-H resonance of furan (6.07 ppm).[15] The free base **7** obtained by deprotonation of **7**-H_2 with TEA preserves the character observed for the dicationic form, but with lowered aromatic character in comparison to **6**. Thus the ^{1}H NMR spectrum of **7** contains three AB systems, with typical scalar coupling constants (ca. 5 Hz) assigned to the β-pyrrolic protons. An upfield relocation of the pyrrole protons (7.85−7.39 ppm) in comparison to the same positions in **7**-H_2, accompanied by downfield relocation of H(21) (**7**-H_2, −0.51; **7**, 2.38 ppm), reflects lowering of the aromatic character in **7**.

One can consider the ^{1}H NMR shifts of the internally located CH proton and the peripheral pyrrole resonances as a convenient spectroscopic criterion of carbaporphyrinoid aromaticity. Under these terms, **7** and **7**-H_2 present a relatively small degree of aromaticity, similar to that detected previously for selected carbaporphyrinoids.[14,23,24]

Coordination of Zn(II) and Cd(II) by *O*-Confused Oxaporphyrin. Insertion of zinc(II), cadmium(II), and nickel(II) into **7** has been readily achieved by boiling a mixture of the free base and an appropriate salt, usually anhydrous chloride, in a chloroform or chloroform/THF solution (Scheme 5).

In all cases, yields are quantitative (see Experimental Section). The resulting complexes will be denoted [(pyr)-*OCPH*]Zn^{II}Cl **7**-ZnCl, [(pyr)*OCPH*]Cd^{II}Cl **7**-CdCl, and [(pyr)*OC*P]Ni^{II} **7**-Ni. Significantly, **7**-Ni was previously obtained by a different route, i.e., by insertion of nickel(II) into **4**.[15] The insertion process was then accompanied by the dehydrogenation step, and the macrocyclic ring that is formed corresponds to the true oxaporphyrin, although it's embedded into its 3-substituted form of **7**. The nickel(II) ion of [(pyr)-*OC*P]Ni^{II} is bound by three pyrrolic nitrogens and a trigonally hybridized C(21) atom of the inverted furan.[15]

In contrast to nickel(II), the zinc(II) and cadmium(II) ions do not form a regular metal−carbon bond (Scheme 5). The macrocycle acts as a monoanionic ligand, and a compensation of the metal charge requires an axial chloride coordination. Three nitrogen atoms and the CH fragment of the inverted furan occupy equatorial positions.

Spectroscopic Characterization of 7-ZnCl and 7-CdCl. The electronic spectra registered for **7**-ZnCl and **7**-CdCl (Figure 3) present complex patterns characteristic for the true

(23) Chmielewski, P. J.; Latos-Grażyński, L.; Głowiak, T. *J. Am. Chem. Soc.* **1996**, *118*, 5690.
(24) Lash, T. D.; Chaney, S. T. *Angew. Chem., Int. Ed.* **1997**, *36*, 839.

Scheme 5. Insertion of Metal Ions

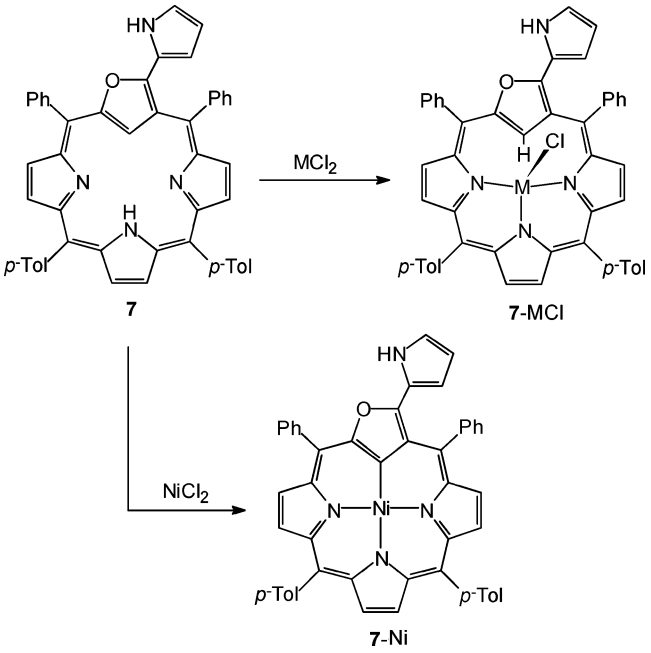

O-confused oxaporphyrin with appended pyrrole or its complexes.[15] The analogical, complex patterns have been observed for **7** and its dicationic form **7**-H_2 (Figure 1) as well. Presumably, the absorption band at ca. 900 nm reflects the conjugation of the appended pyrrole ring with the *O*-confused porphyrin macrocycle.

The ^{1}H NMR spectra observed for **7**-ZnCl and **7**-CdCl are presented in Figure 4. The ^{1}H NMR spectrum of **7**-ZnCl (Figure 4, trace A) shows three AB patterns located according to the COSY map (8.28, 7.75 (^3J = 4.9 Hz); 8.18, 7.84 (^3J = 4.9 Hz); 7.80, 7.77 (^3J = 4.9 Hz)) and assigned to three pyrrole rings. The unique inner C(21)H resonance of the inverted furan ring is located at 0.15 ppm, i.e., slightly upfield with respect to the corresponding (21)H resonance of **7**. The downfield relocation of β-H resonances of **7**-ZnCl as compared to those of **7** suggests some increase of ring current effect due to coordination of the metal ion. The chemical shifts determined for **7**-CdCl resemble those of **7**-ZnCl.

The proximity of the furan fragment to the metal ion induces direct scalar couplings between the spin-active nucleus of the metal ($^{111/113}$Cd) and the adjacent ^{1}H nucleus. Interaction with the spin-active Cd nuclei leads to scalar couplings observed in the ^{1}H NMR spectra of **7**-CdCl. These couplings generate characteristic satellite patterns, which can

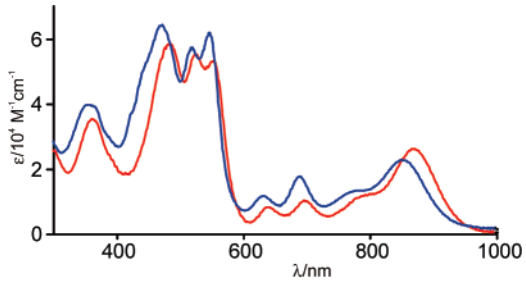

Figure 3. Electronic spectra of **7**-ZnCl (blue) and **7**-CdCl (red) in CH_2Cl_2.

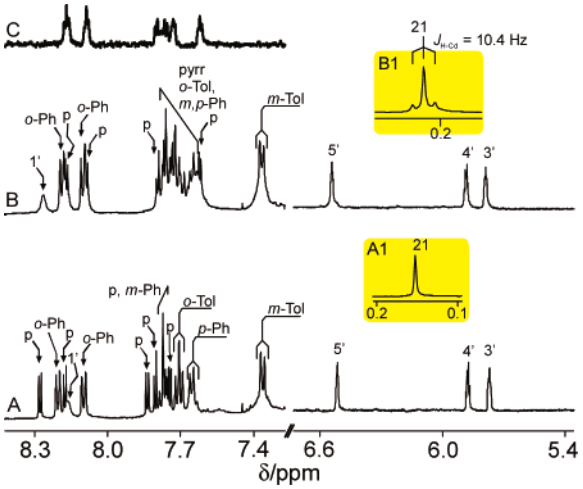

Figure 4. ^{1}H NMR spectra of (A) **7**-ZnCl and (B) **7**-CdCl (chloroform-*d*, 298 K). (C) 1D gsHSQC for **7**-CdCl. Insets (not to scale) A1 and B1 show the H(21) resonance for **7**-ZnCl and **7**-CdCl, respectively. The coupling to $^{111/113}$Cd is marked in inset B1.

be extracted from the 1D spectrum using appropriate filtering techniques (Figure 4, trace C). β-Pyrrolic protons of **7**-CdCl exhibit the usual four-bond couplings to $^{111/113}$Cd (ca. 4.5 Hz), also observed for regular cadmium(II) porphyrins and cadmium(II) benziporphyrins.[8,13,25]

The H(21) pattern displayed by **7**-CdCl is shown in inset B1 of Figure 3. The central line, which corresponds to the molecules containing spin-inactive Cd isotopes, is flanked with a pair of satellites. Significantly, the $^{111/113}$Cd satellites (J = 10.4 Hz) are detected for the (21)H signal (inset B1 of Figure 4). This coupling is too effective to be of the usual through-bond origin, because the metal nucleus and the proton of the inverted furan are five bonds apart and the geometry of the bond path is unfavorable. These couplings are therefore a result of the weak cadmium−(21)H interaction. In structural terms, the detected coupling reflects the spatial proximity between the cadmium ion and the furan fragment. The coupling constant value is slightly larger compared to that of cadmium(II) benziporphyrin.[8]

The interaction of the metal ion and C(21)H is reflected by carbon chemical shifts. The C(21) resonances of **7**-CdCl and **7**-ZnCl have been detected at 78.3 and 81.4 ppm, respectively. Thus they experience a remarkable upfield change relative to free base **7** (101.3 ppm). Analogously, the C(22) signals of the Zn(II), Cd(II), and Hg(II) complexes of *m*-benziporphyrin complexes experience remarkable upfield shifts relative to free base **1** (up to 26.6 ppm). Significantly, the molecular structure of *m*-benziporphyrin complexes supports the side-on interaction between the metal ion and benzene.[8] The proper tetrahedral geometry of an internal carbon is reflected by the characteristic carbon shift (33.4 ppm), as observed for nickel(II) complexes of alkylated[26] and protonated *N*-confused porphyrin.[27]

(25) Jakobsen, H. J.; Ellis, P. D.; Inners, R. R.; Jensen, C. F. *J. Am. Chem. Soc.* **1982**, *104*, 7742.
(26) Schmidt, I.; Chmielewski, P. J. *Chem. Commun.* **2002**, 92.
(27) Schmidt, I.; Chmielewski, P. J.; Ciunik, Z. *J. Org. Chem.* **2002**, *67*, 8917.

Table 1. ^{1}H (^{13}C) NMR Chemical Shift Values Observed for the Appended Pyrrole Ring

	3′	4′	5′	21
pyrrole	6.22 (108.2)	6.22 (108.2)	6.68 (118.5)	
6	5.53 (107.3)	5.93 (108.9)	6.45 (116.5)	−5.55 (111.8)
7	6.64 (124.6)	6.17 (114.7)	6.97 (131.9)	−0.41 (101.3)
7-H_2	6.10 (116.5)	6.00 (111.2)	6.56 (123.8)	2.39 (109.1)
7-Ni[15]	6.34 (119.2)	6.17 (111.9)	6.76 (126.4)	
7-ZnCl	5.82 (117.1)	5.88 (111.5)	6.52 (124.3)	0.17 (81.8)
7-CdCl	5.80 (116.2)	5.89 (111.0)	6.54 (123.6)	0.21 (78.3)
dipyrromethene	6.64 (128.8)	6.39 (117.2)	7.63 (143.1)	

The analysis of the ^{13}C chemical shifts registered for the appended pyrrole ring of **7**-ZnCl and **7**-CdCl (Table 1) provides essential insight into the different roles of the pyrrole fragment, underscoring the direct electronic effects.

The ring-current contributions to overall changes in ^{13}C chemical shifts are negligible. For the sake of comparison, the respective chemical shift values of the free pyrrole and the conjugated pyrrole ring of 5-anisol-dipyrromethene[15] have been included in Table 1. These values set the spectroscopic standards for two extreme structures of the appended pyrrole. The analysis of the ^{13}C chemical shifts registered for the appended pyrrole ring of **7**-ZnCl and **7**-CdCl (Table 1) suggests an effective conjugation between the macrocycle and appended pyrrole moiety. In terms of ^{13}C chemical shifts, it is clear that the extent of the conjugation resembles one characteristic for [(pyr)*O*CP]Ni^{II}.[15]

The remarkable changes of the appended pyrrole ^{1}H NMR pattern have been observed in the analyzed **7**-H_2, **7**, **7**-ZnCl, and **7**-CdCl series (Table 1). The marked upfield relocation of the **7**-ZnCl and **7**-CdCl resonances with respect to **7**-H_2 or **7** is the most analytically important. As shown by the X-ray study, the macrocycle of **7**-Ni is only slightly distorted from planarity.[15] The dihedral angle between the macrocyclic and appended pyrrole plane reflects the biphenyl-like arrangement and equals 26.4°. The DFT calculations afford a similar structure for **7**. The visible puckering of the macrocycle and the large tilt of furan have been found in the optimized structure of **7** (see below). Thus the reasons for the ^{1}H NMR chemical shift changes are complex, as the simultaneous modification of the macrocyclic ring current and the molecular structure of the furan-appended pyrrole fragment are important.

DFT Studies. In metal complexes **7**-ZnCl and **7**-CdCl, the reasonable conformation of the macrocycle has the furan ring tilted away from the metal center, with the inner CH bonds and the axial MCl bond in an anti orientation. The observation of scalar coupling between the Cd nucleus and H(21) in **7**-CdCl indicates that there must be a certain accumulation of electron density between the metal and furan to transmit the coupling. This observation indicates that the furan fragment approaches the cadmium ion at a distance much shorter than the sum of the van der Waals radii. To approach this problem, we have applied the density functional theory (DFT) in a way similar to that previously described for *m*-benziporphyrin and *p*-benziporphyrin complexes.[8,28]

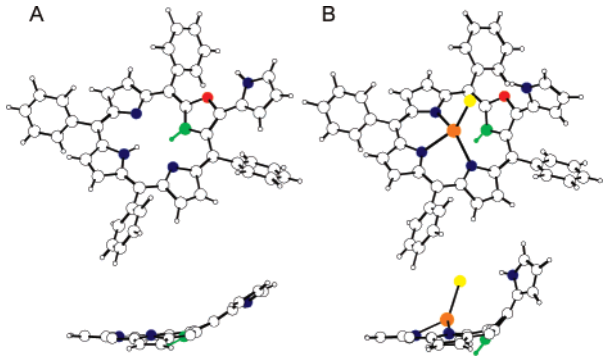

Figure 5. DFT calculated geometries of **7** (A) and **7**-CdCl (B). The upper traces present the perspective projection, whereas the bottom one shows the side view (aryl groups omitted for clarity). The **7**-ZnCl structure is nearly identical to that of the cadmium compound (see text for details).

Here, we have performed the DFT calculations for **7**-ZnCl and **7**-CdCl. We have found it necessary to include in calculations *m*-aryl substituents despite a required substantial computational effort. Previously, we found that the absence of *m*-aryl produces substantial differences in the optimized macrocyclic geometry.[8,28,29] For comparison, we have carried out the DFT optimization (B3LYP/6-31G**) of the free base **7**. NICS (nucleus-independent chemical shift) values[30−36] have been determined for the optimized structures **7** at a center of the porphyrinoid crevice. The global NICS value for **7** is −2.42 ppm (the value at 1 Å above the center is −2.98 ppm), consistent with the observation that the diatropic effect in ^{1}H NMR is relatively small.

The two DFT-optimized structures **7**-ZnCl and **7**-CdCl (B3LYP/LANL2DZ) are very similar (Figure 5). The optimized structural parameters are contained in the Supporting Information. The Cd ion in **7**-CdCl is displaced from the N_3 plane by ca. 0.51 Å toward the chloride. A slightly smaller displacement has been found for zinc(II) of **7**-ZnCl (0.18 Å). The degrees of tilt adopted by the furan moieties in **7**-ZnCl (48.9°) and **7**-CdCl (49.0°) as expressed by the C_4O/N_3 dihedral angles (given in parentheses) are remarkably large as compared to that of the crystal structure of **7**-Ni (5.7°)[15] or the DFT-optimized structure of **7** (23.2°).

The optimized bond lengths (see the Supporting Information) resemble those found by X-ray crystallography for zinc(II) and cadmium(II) carbaporphyrins.[8,13,37] The dihedral angles between furan and appended pyrrole equal 38.8° and 41.4° for **7**-ZnCl and **7**-CdCl, respectively. The optimized M···C(21) and M···H(21) distances are 2.73 and 2.81 Å for Cd(II), and 2.70 and 2.71 Å for Zn(II), respectively. The distances resemble those determined by X-ray structure for cadmium(II) *m*-benziporphyrin, in which scalar coupling was

(28) Stępień, M.; Latos-Grażyński, L.; Szterenberg, L. *Inorg. Chem.* **2004**, *43*, 6654.
(29) Szterenberg, L.; Latos-Grażyński, L. *THEOCHEM* **1999**, *490*, 33.
(30) Schleyer, P. v. R.; Meaerker, C.; Dransfeld, A.; Jiao, H.; Hommes, N. J. R. v. E. *J. Am. Chem. Soc.* **1996**, *118*, 6317.
(31) Cyrański, M. K.; Krygowski, T. M.; Wisiorowski, M.; Hommes, N. J. R. v. E.; Schleyer, P. v. R. *Angew. Chem., Int. Ed.* **1998**, *37*, 177.
(32) Schleyer, P. v. R.; Manoharan, M.; Wang, Z.-X.; Kiran, B.; Jiao, H.; Puchta, R.; Hommes, N. J. R. v. E. *Org. Lett.* **2001**, *3*, 2465.
(33) Krygowski, T. M.; Cyrański, M. K. *Chem. Rev.* **2001**, *101*, 1385.
(34) Furuta, H.; Maeda, H.; Osuka, A. *J. Org. Chem.* **2001**, *66*, 8563.
(35) Kawase, T.; Oda, M. *Angew. Chem., Int. Ed.* **2004**, *43*, 4396.
(36) Okazaki, T.; Laali, K. L. *J. Org. Chem.* **2004**, *69*, 510.
(37) Furuta, H.; Ishizuka, T.; Osuka, A. *J. Am. Chem. Soc.* **2002**, *124*, 5622.

also detected.[8] A shorter distance was determined for the zinc(II) *N*-confused porphyrin complex (2.49 Å).[37−39] The Cd···C(21) distance in **7**-CdCl exceeds the typical Cd−C bond length (2.10−2.35 Å),[40] but is much shorter than the corresponding van der Waals contact (3.3 Å).[41] Similarly, the Zn···C(21) distance in **7**-ZnCl exceeds the typical Zn−C bond length (1.984−1.987 Å),[40,42] but is much shorter than the corresponding van der Waals contact (3.1 Å).[41]

Conclusion

In the present work, we have described the isolation and reactivity of the true *O*-confused oxaporphyrin, albeit with an appended pyrrole ring covalently linked at the C(3) position. The pyrrole-appended *O*-confused oxaporphyrin molecule, applied as a ligand toward nickel(II), zinc(II), and cadmium(II) metal ions, reveals the peculiar plasticity of its molecular and electronic structure. The insertion of nickel(II) was accompanied by the dehydrogenation step, and the macrocyclic ring formed corresponds to the true oxaporphyrin, although it's embedded into its 3-substituted form. The nickel(II) ion is bound by three pyrrolic nitrogens and a trigonally hybridized C(21) atom of the inverted furan. In contrast, the zinc(II) and cadmium(II) ions favor the different coordination mode of oxacarbaporphyrin. Namely, the macrocycle acts as a monoanionic ligand, and three nitrogen atoms and the CH fragment of the inverted furan occupy equatorial positions. Essentially, the oxidation state and the size of the central metal ion can be considered to be a factor that determines the molecular structure of the ligand. The monoanionic, dianionic, or trianionic macrocyclic core of pyrrole-appended derivatives has been favored to match requirements of zinc(II), cadmium(II), nickel(II), palladium(II), and silver(III).

In the present paper, we have described spectroscopic manifestations of the side-on metal−arene interactions observed in the diamagnetic Zn(II) and Cd(II) complexes. The metal−furan interaction leads to scalar coupling between the spin-active metal nucleus (^{111}Cd, ^{113}Cd) and the proximate ^{1}H and ^{13}C nuclei of the arene.

Experimental Section

Solvents and Reagents. Chloroform-*d* and dichloromethane-d_2 (both CIL) were used as received. The starting macrocycle **4** (5,20-diphenyl-10,15-ditolyl-2-oxa-3-hydro-3-(2′-pyrrolilo)-21-carbaporphyrin) was obtained as previously described.[15]

5,20-Diphenyl-10,15-ditolyl-2-oxa-3-ethoxy-3-(2′-pyrrolilo)-21-carbaporphyrin 6. In a round-bottom flask, 10 mg of **4** was dissolved in 30 mL of ethanol. To that solution was added metallic sodium (7 mg), and the obtained mixture was refluxed for an additional 30−40 min. After that time, the solvent was removed with a vacuum rotary evaporator. The solid residue was dissolved in a small volume of fresh distilled dichloromethane and evaporated (two times). The remaining green solid was dissolved in fresh distilled dichloromethane, and was filtered. The obtained solution was purified with a chromatographic column filled with aluminum oxide (GII). The fast-moving brown fraction was collected and evaporated to give **6** with quantitative yield. ^{1}H NMR (500.13 MHz, CD_2Cl_2): δ 8.58 (d, 1H, ^{3}J = 4.6 Hz), 8.56 (d, 1H, ^{3}J = 4.6 Hz), 8.55 (d, 1H, ^{3}J = 4.6 Hz), 8.53 (d, 1H, ^{3}J = 4.6 Hz), 8.51 (d, 1H, ^{3}J = 4.9 Hz), 8.20 (d, 1H, ^{3}J = 4.9 Hz), 8.14 (m, 3H), 8.06 (d, 1H, ^{3}J = 8 Hz), 8.03−7.97 (m, 3H), 7.9 (d, 1H, ^{3}J = 8 Hz), 7.72 (t, 2H), 7.65−7.49 (m, 9H), 7.25 (m, 1H), 6.92 (d, 1H, ^{3}J = 8 Hz), 6.49 (m, 1H), 5.90 (m, 1H), 5.39 (m, 1H), 3.86 (m, 1H), 3.35 (m, 1H), 2.68 (s, 3H), 2.66 (s, 3H), 1.21 (t, 3H), −5.55 (s, 1H). ^{13}C NMR (125.7 MHz, $CDCl_3$): δ 156.2, 153.4, 152.9, 140.5, 139.7, 139.5, 139.45, 139.4, 139.0, 138.7, 137.5, 137.4, 135.7, 134.9, 134.5, 134.3, 134.2, 133.7, 133.4, 133.1, 132.7, 132.4, 128.0, 127.75, 127.72, 127.70, 127.5, 127.1, 126.4, 126.2, 126.0, 125.9, 124.5, 123.8, 121.1, 120.2, 116.3, 114.8, 111.8, 108.7, 107.1, 106.1, 105.1, 105.0, 58.9, 21.7, 21.7, 15.2. UV−vis (λ_{max} (nm), log ϵ): 433 (4.71), 528 (2.63), 562 (2.49), 613 (2.27), 669 (2.42). HRMS (ESI, *m*/*z*): calcd for [$C_{52}H_{42}N_4O_2$ + H^+], 755.3386; found, 755.3381.

5,20-Diphenyl-10,15-ditolyl-2-oxa-3-(2′-pyrrolyl)-21-carbaporphyrin Dication 7-H$_2$. 6 (10 mg) was dissolved in 15 mL of fresh distilled dichloromethane. The concentrated TFA was added until the distinct color change from brown to violet was observed. The crude product was recrystallized with CH_2Cl_2/hexane to give **7**-H_2 with almost quantitative yield (up to 97%). ^{1}H NMR (500.13 MHz, CD_2Cl_2): δ 9.34 (bs, 1H), 8.51 (d, 2H, ^{3}J = 7.3 Hz), 8.43 (d, 2H, ^{3}J = 7.3 Hz), 8.34 (d, 1H, ^{3}J = 4.6 Hz), 8.33 (d, 1H, ^{3}J = 4.9 Hz), 8.08−8.01 (m, 6H), 7.99 (d, 1H, ^{3}J = 4.6 Hz), 7.98−7.93 (m, 4H), 7.92−7.79 (m, 7H), 7.67−7.62 (m, 4H), 6.98 (m, 1H), 6.67 (m, 1H), 6.17 (m, 1H), 2.67 (s, 3H), 2.66 (s, 3H), −0.51 (s, 1H). ^{13}C NMR (125.7 MHz, CD_2Cl_2): δ 152.2, 150.2, 149.8, 148.9, 148.1, 147.3, 146.2, 144.9, 141.6, 141.2, 140.9, 140.5, 138.8, 138.4, 137.1, 136.9, 139.7, 136.6, 135.7, 132.5, 131.8, 131.6, 131.4, 130.5, 130.4, 130.2, 129.5, 129.3, 129.1, 129.0, 128.7, 128.2, 124.8, 123.5, 122.8, 121.1, 117.2, 116.1, 114.9, 113.9, 101.1, 21.7, 21.6. UV−vis (λ_{max} (nm), log ϵ): 356 (3.91), 389 (3.98), 444 (4.17), 472 (4.13), 533 (4.11), 573 (4.18), 652 (3.58), 708 (3.52), 911 (3.39). HRMS (ESI, *m*/*z*): calcd for [$C_{50}H_{36}N_4O$ + H^+], 709.2967; found, 709.2962.

7. ^{1}H NMR (500.13 MHz, $CDCl_3$): δ 8.00 (m, 2H), 7.97 (m, 3H), 7.85 (d, 1H, ^{3}J = 4.9 Hz), 7.80 (d, 1H, ^{3}J = 4.6 Hz), 7.67−7.57 (m, 13H), 7.48 (d, 1H, ^{3}J = 4.6 Hz), 7.39 (d, 1H, ^{3}J = 4.6 Hz), 7.35 (m, 4H), 6.56 (m, 1H), 6.10 (m, 1H), 6.00 (m, 1H), 4.47 (bs, 1H), 2.53 (s, 6H), 2.39 (s, 1H). UV−vis (λ_{max} (nm), log ϵ): 360 (4.04), 420 (4.18), 449 (4.15), 502 (4.17), 528 (sh), 627 (3.46), 681 (3.77), 809 (3.29), 883 (3.17).

5,20-Diphenyl-10,15-ditolyl-2-oxa-3-(2′-pyrrolyl)-21-carbaporphyinato Chlorozinc(II) 7-ZnCl. 7 (10 mg) was dissolved in 15 mL of chloroform with a small amount of fresh distilled triethylamine (2 drops). Zinc(II) chloride (excess) was added in a small volume of fresh distilled THF. After 20 min, the resulting mixture was washed with water (3 × 20 mL). The organic layer was dried with Na_2SO_4, filtered, and evaporated with a vacuum rotary evaporator. The crude product was recrystallized with $CHCl_3$/hexane to gave **7**-ZnCl with quantitative yield. ^{1}H NMR (500.13 MHz, $CDCl_3$): δ 8.28 (d, 1H, ^{3}J = 4.9 Hz), 8.20 (d, 2H, ^{3}J = 7.3 Hz), 8.17 (d, 1H, ^{3}J = 4.9 Hz), 8.1 (bs, 1H), 8.09 (d, 1H, ^{3}J = 7.3 Hz), 7.84 (d, 1H, ^{3}J = 4.6 Hz), 7.8 (d, 1H, ^{3}J = 4.9 Hz), 7.79−7.75 (m, 1H), 7.74 (d, 1H, ^{3}J = 4.9 Hz), 7.73−7.68 (m), 7.67−7.62 (m), 7.38−7.34 (m, 4H), 6.52 (m, 1H), 5.88 (m, 1H), 5.77 (m, 1H), 2.55 (2xs, 6H), 0.15 (s, 1H). ^{13}C NMR (125.7 MHz,

(38) Furuta, H.; Ishizuka, T.; Osuka, A. *Inorg. Chem. Commun.* **2003**, *6*, 398.
(39) Furuta, H.; Morimoto, T.; Osuka, A. *Inorg. Chem.* **2004**, *43*, 1618.
(40) Hursthouse, M. B.; Motevalli, M.; O'Brien, P.; Walsh, J. R.; Jones, A. C. *Organometallics* **1991**, *10*, 3196.
(41) Bondi, A. *J. Phys. Chem.* **1964**, *68*, 441.
(42) Dekker, J.; Boersma, J.; Fernholt, L.; Haaland, A.; Spek, A. L. *Organometallics* **1987**, *6*, 1202.

$CDCl_3$): δ 162.7, 161.2, 157.4, 157.1, 152.8, 152.6, 148.8, 148.4, 140.8, 138.3, 137.9, 137.4, 137.2, 135.9, 135.4, 135.0, 134.4, 133.7, 133.5, 133.4, 132.8, 129.7, 129.3, 129.1, 128.9, 128.0, 127.9, 126.1, 125.1, 123.9, 122.6, 120.1, 118.3, 118.2, 116.6, 111.2, 81.4, 21.4. UV−vis (λ_{max} (nm), log ϵ): 357 (4.60), 469 (4.81), 518 (4.76), 546 (4.79), 631 (4.07), 689 (4.25), 771 (3.99), 851 (4.36). HRMS (ESI, *m*/*z*): calcd for $C_{50}H_{35}N_4OZn^+$, 771.2102; found, 771.2097.

5,20-Diphenyl-10,15-ditolyl-2-oxa-3-(2′-pyrrolyl)-21-carbaporphyrinato Chlorocadmium(II) 7-CdCl. **7** (10 mg) was dissolved in 15 mL of chloroform with a small amount of fresh distilled triethylamine (2 drops). Cadmium(II) chloride (excess) was added, and the resulting mixture was refluxed for the next 30 min. After that time, the solvent was removed with a vacuum rotary evaporator. The remaining solid was dissolved in 20 mL of fresh distilled dichloromethane, and washed with water (3 × 20 mL). The organic layers were dried with Na_2SO_4, filtered, and evaporated. The crude product was recrystallized with $CHCl_3$/hexane to give **7**-CdCl with quantitative yield. ^{1}H NMR (500.13 MHz, $CDCl_3$): δ 8.28 (bs, 1H), 8.21−8.15 (m, 3H), 8.12−8.08 (m, 3H), 7.81−7.61 (m, 14H), 7.40−7.35 (m, 4H), 6.54 (m, 1H), 5.89 (m, 1H), 5.79 (m, 1H), 2.55 (s, 6H), 0.21 (t, 1H, J_{H-Cd} = 10.4 Hz). ^{13}C NMR (125.7 MHz, $CDCl_3$): δ 164.2, 162.4, 160.1, 159.5, 153.9, 153.5, 148.3, 141.0, 138.9, 138.6, 137.9, 137.5, 136.2, 135.8, 135.4, 135.0, 134.9, 134.8, 134.6, 133.9, 133.5, 129.7, 129.5, 129.3, 128.6, 128.3, 125.8, 124.1, 122.8, 119.9, 119.6, 116.7, 111.5, 78.3, 21.8. UV−vis (λ_{max} (nm), log ϵ): 362 (4.55), 483 (4.76), 525 (4.74), 551 (4.73), 639 (3.92), 697 (4.01), 785 (4.07), 868 (4.42). **MS** (ESI, *m*/*z*): calcd for $C_{50}H_{35}N_4O^{112}Cd^+$, 819.3; found, 819.1.

5,20-Diphenyl-10,15-ditolyl-2-oxa-3-(2′-pyrrolyl)-21-carbaporphyrinato Nickel(II) 7-Ni. **7** (10 mg) was dissolved in 15 mL of chloroform with a small amount of fresh distilled triethylamine (2 drops). To the resulting mixture was added nickel(II) chloride (excess) dissolved in 10 mL of methanol, and the resulting mixture was stirred for an additional 12 h. After that time, the solvent was removed with a vacuum rotary evaporator. The remaining solid was dissolved in a small amount of fresh distilled dichloromethane, filtered, and chromatographed with silica gel (Mesh 35−70). The fast-moving green fraction was collected, and was recrystallized with $CHCl_3$/MeOH to gave **7**-Ni (yield 60%). The complex presents spectroscopic properties identical to those previously described.[15]

Instrumentation. NMR spectra were recorded on a Bruker Avance 500 spectrometer (frequencies: ^{1}H 500.13 MHz, ^{13}C 125.77 MHz, ^{113}Cd 106.05 MHz) equipped with either a broadband inverse gradient probehead or a direct broadband probehead. A 1D variant of a gradient-selected HSQC sequence was employed to record the ^{113}Cd-filtered spectra, with evolution times optimized for the observed range of coupling constants. Absorption spectra were recorded on a diode array Hewlett-Packard 8453 spectrometer. Mass spectra were recorded on an AD-604 spectrometer using the electrospray and liquid matrix secondary-ion mass spectrometry techniques.

DFT Calculations. DFT calculations for structures **7**, **7**-CdCl, and **7**-ZnCl were performed with the GAUSSIAN03 program.[43] Geometry optimizations were carried out within unconstrained *C*1 symmetry. Becke's three-parameter exchange functional[44] with the gradient-corrected correlation formula of Lee, Yang, and Parr (DFT-(B3LYP))[45] was used with the LANL2DZ basis set for metal complexes,[46] and with 6-31G** for the free base **7**. Harmonic vibrational frequencies were calculated for **7** (6-31G**), **7**-ZnCl, and **7**-CdCl (LANL2DZ) using analytical second derivatives, in order to establish the nature of the stationary points. All structures were found to have converged to a minimum on the potential-energy surface.

To probe the ring current in **7**, we calculated the nucleus-independent chemical shift (NICS) (HF/6-31G**/B3LYP/6-31G**).

Acknowledgment. This work was supported by the Ministry of Scientific Research and Information Technology of Poland under Grant 3 T09A 162 28. DFT calculations were preformed at the Supercomputer Centers in Wrocław and Poznań.

Supporting Information Available: Bond lengths for DFT optimized geometry and optimized structural parameters of **7**, **7**-CdCl, and **7**-ZnCl. This material is available free of charge via the Internet at http://pubs.acs.org.

IC051238X

(43) Frisch, M. J.; Trucks, G. W.; Schlegel, H. B.; Scuseria, G. E.; Robb, M. A.; Cheeseman, J. R.; Montgomery, J. A., Jr.; Vreven, T.; Kudin, K. N.; Burant, J. C.; Millam, J. M.; Iyengar, S. S.; Tomasi, J.; Barone, V.; Mennucci, B.; Cossi, M.; Scalmani, G.; Rega, N.; Petersson, G. A.; Nakatsuji, H.; Hada, M.; Ehara, M.; Toyota, K.; Fukuda, R.; Hasegawa, J.; Ishida, M.; Nakajima, T.; Honda, Y.; Kitao, O.; Nakai, H.; Klene, M.; Li, X.; Knox, J. E.; Hratchian, H. P.; Cross, J. B.; Adamo, C.; Jaramillo, J.; Gomperts, R.; Stratmann, R. E.; Yazyev, O.; Austin, A. J.; Cammi, R.; Pomelli, C.; Ochterski, J. W.; Ayala, P. Y.; Morokuma, K.; Voth, G. A.; Salvador, P.; Dannenberg, J. J.; Zakrzewski, V. G.; Dapprich, S.; Daniels, A. D.; Strain, M. C.; Farkas, O.; Malick, D. K.; Rabuck, A. D.; Raghavachari, K.; Foresman, J. B.; Ortiz, J. V.; Cui, Q.; Baboul, A. G.; Clifford, S.; Cioslowski, J.; Stefanov, B. B.; Liu, G.; Liashenko, A.; Piskorz, P.; Komaromi, I.; Martin, R. L.; Fox, D. J.; Keith, T.; Al-Laham, M. A.; Peng, C. Y.; Nanayakkara, A.; Challacombe, M.; Gill, P. M. W.; Johnson, B.; Chen, W.; Wong, M. W.; Gonzalez, C.; Pople, J. A. *Gaussian 03,* revision C. 01; Gaussian, Inc.: Pittsburgh, PA, 2004.
(44) Becke, A. D. *Phys. Rev. A* **1988**, *38*, 3098.
(45) Lee, C.; Yang, W.; Parr, R. G. *Phys. Rev. B* **1988**, *37*, 785.
(46) Hay, P. J.; Wadt, W. R. *J. Chem. Phys.* **1985**, *82*, 270, 284, 299.